Carbohydrate Polymers 80 (2010) 442–448

Contents lists available at ScienceDirect

Carbohydrate Polymers

journal homepage: www.elsevier.com/locate/carbpol

Folate conjugated carboxymethyl chitosan–manganese doped zinc sulphide nanoparticles for targeted drug delivery and imaging of cancer cells

Manjusha Elizabeth Mathew [a], Jithin C. Mohan [a], K. Manzoor [a], S.V. Nair [a], H. Tamura [b], R. Jayakumar [a,*]

[a] Amrita Centre for Nanosciences and Molecular Medicine, Amrita Institute of Medical Sciences and Research Centre, Amrita Vishwa Vidyapeetham University, Kochi 682 026, India
[b] Faculty of Chemistry, Materials and Bioengineering & High Technology Research Centre, Kansai University, Osaka 564-8680, Japan

ARTICLE INFO

Article history:
Received 2 November 2009
Received in revised form 25 November 2009
Accepted 27 November 2009
Available online 2 December 2009

Keywords:
Folate receptor
Targeting
Manganese doped zinc sulphide
Cancer cells
Imaging
Drug delivery
Carboxymethyl chitosan

ABSTRACT

We developed a novel folic acid (FA) conjugated carboxymethyl chitosan coordinated to manganese doped zinc sulphide quantum dot (FA–CMC–ZnS:Mn) nanoparticles. The system can be used for targeting, controlled drug delivery and also imaging of cancer cells. The prepared nanoparticles were characterized using SEM, AFM, FT-IR, UV and DLS studies. The size range of 5-FU encapsulated FA–CMC–ZnS:Mn nanoparticles were from 130 to 150 nm. The anticancer drug selected in this study was 5-Fluorouracil which can be used for the breast cancer treatment. The nontoxicity of FA–CMC–ZnS:Mn nanoparticles were studied using L929 cells. Breast cancer cell line MCF-7 was used to study the imaging, specific targeting and cytotoxicity of the drug loaded nanoparticles. The *in vitro* imaging of cancer cells with the nanoparticles studied using fluorescent microscopy. The bright and stable luminescence of quantum dots can be used to image the drug carrier in cancer cells without affecting their metabolic activity and morphology.

1. Introduction

Multi-functional nanoparticles are now became alternative system for drug delivery which has great potential for cancer therapy. Nanoparticles offer opportunities for multi-functionalization to allow for the targeted delivery of drugs with imaging agents. Polymeric nanocarriers can provide versatile platforms for the delivery of multiple pharmacological agents, specifically to enhance therapeutic effect and overcome drug resistance in cancer (Jabr-Milane et al., 2008; Prabaharan, Grailer, Pilla, Steeber, & Gong, 2009a; Prabaharan, Grailer, Pilla, Steeber, & Gong, 2009b; Prabaharan, Grailer, Pilla, Steeber, & Gong, 2009c; Prabaharan, Grailer, Steeber, & Gong, 2009d; Saad et al., 2008; Sanvicens & Marco, 2008; Shen et al., 2008; Soppimath, Aminabhavi, Kulkarni, & Rudzinski, 2000). Commonly defined nanoparticle carriers include: liposomes, micelles, dendrimers, solid lipid, metallic, semiconductor and polymeric nanoparticles (Vlerken & Amiji, 2006; Wu, Liu, & Lee, 2006). Derivatives of chitosan have been developed to overcome its disadvantages like limited solubility and lack of effectiveness as absorption enhancer at neutral pH values (Jayakumar, Nme, Tokura, & Tamura, 2007; Jayakumar, Prabaharan, Reis, & Mano, 2005; Prabaharan, 2008; Prabaharan & Mano, 2005). CMC is a water-soluble chitosan derivative in which the $-CH_2OH$ group of each monomer substituted by –COOH group (Ke, Mathias, & Green, 2003).

Semiconductor nanoparticles called quantum dots are a prominent class of nanoparticle imaging agents. Unlike organic dye probes, QDs are characterized by large stokes shifts, broad absorption bands and narrow size dependent emission bands. Moreover, the QDs are usually a few nanometers in size. The size dependent emission of QDs is the result of quantum confinement effect (Lu & Low, 2002). ZnS:Mn QDs shows enhanced emission efficiencies (Fernando & Sérgio, 2004). In the case of ZnS QDs doped with Mn isoelectronic impurities, the Mn^{2+} ion d-electron states acts as efficient luminescent centers while electronic interaction with host nanocrystal leads to high luminescent efficiencies at room temperature (Michael, David, Eric, & Christof, 2008). In our study the anticancer drug 5-Fluorouracil (5-FU) was used. This is an established drug for chemotherapy for decades. Some of its principal uses are in colorectal, pancreatic, breast, head and neck cancer (Steitz, Hofmann, Axmann, & Petri-Fink, 2008). Tumor cell targeting enhances the therapeutic potential of chemotherapy agents. The cell-membrane folate receptor was a potential molecular target for tumor-selective drug delivery (Bhargava, Gallagher, & Welker, 1994; Xie, Liu, & Zhan, 2005). The attractiveness of folate has been enhanced by its high binding affinity, low immunogenicity and ease of modification. It is upregulated in many human cancers such as ovary, brain, kidney, breast, myeloid cells and lung (Manzoor, Johny, Menon, & Nair, 2009; Pan & Feng, 2009; Shi, Du, Yang, Zhong, & Sun, 2006; Zhu et al., 2007).

* Corresponding author. Tel.: +91 484 2801234; fax: +91 484 2802020.
E-mail addresses: rjayakumar@aims.amrita.edu, jayakumar77@yahoo.com (R. Jayakumar).

0144-8617/$ - see front matter © 2009 Elsevier Ltd. All rights reserved.
doi:10.1016/j.carbpol.2009.11.047

In this paper we are reporting about the synthesis, characterization, drug delivery and cancer cell imaging of novel FA–CMC–ZnS:Mn nanoparticles. The polymeric carrier, CMC as well as the imaging agent, ZnS:Mn were in nanoscale dimensions. This study becomes important in the field of anticancer drug delivery because it aims controlled drug delivery using CMC at the same time imaging the path of this drug carrier system with the help of fluorescence from ZnS:Mn quantum dot. The purpose of this study was to develop such a system by a simple wet chemistry route. Conjugation of CMC with folic acid enables specific targeting of the nanoparticles to cancer cells, which increases the bioavailability of 5-FU.

2. Materials and methods

2.1. Chemicals

Carboxymethyl chitosan (CMC) was purchased from Koyo Chemical Co. Ltd., Japan. The degree of deacetylation and degree of substitution of the polymer were 61.8% and 0.54% respectively. Zinc acetate (98+%), manganese sulfate (98+%), sodium sulfide (98+%), calcium chloride (98+%) were purchased from Sigma–Aldrich (St. Louis, MO, USA). *N*-(3-Dimethyl aminopropyl)-*N*′-ethylcarbodiimide hydrochloride (EDC), *N*-hydroxysuccinimide (NHS), 2,4-dihydroxy-5-fluorpyrimidin (5-FU) were purchased from Aldrich Chemical Company. Folic acid was a kind gift from Micro labs, Bangalore. Breast cancer cells lines MCF-7 and Mouse fibroblast cells L929 obtained from National Centre for Cell Science (Pune, India). Minimal essential medium, fetal bovine serum, penicillin/streptomycin was obtained from GIBCO-BRL (Gaithersburg, MD).

2.2. Formulation of folate conjugated CMC

Three milli-liters of 1 mg/ml solution of folic acid in deionised water was prepared. The surface carboxyl groups of folic acid were activated by adding 0.78 mg of NHS and 0.98 mg of EDC and stirred well at room temperature for 2 h. 5 ml of 5 mg/ml CMC was added to this drop-by-drop with stirring. The reaction was allowed to take place for 8 h.

2.3. Preparation of drug free and drug loaded CMC nanoparticles

The FA–CMC nanoparticles were prepared by ionic cross-linking with $CaCl_2$. $CaCl_2$ solution of concentration 10 mg/ml added slowly to FA–CMC solution under mild magnetic stirring till a stable colloidal solution was obtained. 5-FU encapsulated nanoparticles were prepared in the same way. The 5-FU solution dissolved in methanol was added slowly to FA–CMC solution and stir for 4–5 h up to evaporation of methanol. $CaCl_2$ was added drop-by-drop to form the nanoparticles. The FA–CMC and 5-FU were taken in 2:1 M ratio.

2.4. Synthesis of highly luminescent ZnS:Mn Quantum dots

Ten milli-liters of 0.1 M zinc acetate solution was taken and 1.5 ml of (15 at.%) Manganese sulphate was added to it drop-by-drop under ultrasonication. Then 10 ml of sodium sulfide was added drop-by-drop to this Zn–Mn precursor with stirring. A white colloid of ZnS:Mn was formed immediately after Na_2S addition. The formed solution was exposed to microwave irradiation for 1 min. The resulting solution was then ultrasonicated for 2 min and then stirred for 30 min. The ZnS:Mn colloidal solution was added drop-by-drop (1 drop/minute) to 10 ml of 5-FU encapsulated FA–CMC nanoparticle with ultrasonication until sufficient fluorescence was obtained. The fluorescence from the sample was observed using a UV lamp providing 365 nm excitation energy. The colloidal sample showed orange red emission, typical for Mn^{2+} luminescent centers in ZnS.

2.5. Drug encapsulation efficiency

The final yellowish product was centrifuged at 14,000 rpm for 30 min. The supernatant containing unencapsulated drug was removed. The samples were washed with deionised water. The obtained pellets were then re-suspended in deionised water and freeze dried for two days to get the powdered sample. 3 ml of the supernatant obtained during the centrifugation was taken in a cuvette and the absorbance value at and 266 nm was recorded with a UV Spectrophotometer (Shimadzu UV-1700 Pharma Spec). From this absorbance value, the concentration of free drug was calculated using the standard curve prepared for 5-FU.

$$\text{Encapsulation efficiency } (\%) = \frac{[\text{Drug}]_{\text{tot}} - [\text{Drug}]_{\text{free}}}{[\text{Drug}]_{\text{tot}}}$$

2.6. Surface morphology of the nanoparticles

The surface morphology of 5-FU encapsulated FA–CMC–ZnS:Mn nanoparticles were characterized using Scanning Electron Microscope (SEM) and Atomic Force Microscope (AFM).

2.6.1. SEM

The SEM pictures of 5-FU encapsulated FA–CMC–ZnS:Mn nanoparticles were taken by Scanning Electron Microscope (JEOL, JSPM-6490, Japan). Twenty micro-liters of nanoparticle suspension was diluted with ultra pure water and ultra sonicated for 25 min and 4–5 very small drops deposited on a stub. The drops were dried under Halogen lamp and the images were taken.

2.6.2. AFM

The AFM pictures of 5-FU encapsulated FA–CMC–ZnS:Mn nanoparticles were taken by AFM (JEOL JSPM-5200, Japan) running in noncontact ac mode. 20 μl of nanoparticle suspension was diluted with ultrapure water and sonicated for 25 min and a drop was deposited on a glass thin layer fixed on a metallic magnetic support. The drop was dried under Halogen lamp and the images were taken.

2.6.3. Nanoparticles size and surface charge

DLS instrument (PSS NICOMP Particle Sizing System, Santa Barbara, California) was used to measure the average size and size distribution of the nanoparticles. The zeta potential of nanoparticles was measured using zeta potential analyzer (NICOMP 380 ZLS Zeta Potential/Particle Sizer, Santa Barbara, California). For zeta potential measurements, the samples were diluted with distilled water and placed in the electrophoretic cell. All measurements were performed in triplicate and the standard deviation was recorded.

2.6.4. UV Spectroscopy

The absorbance studies were carried out using UV Spectrophotometer (Shimadzu UV-1700 Pharma Spec). The 5-FU encapsulated FA–CMC–ZnS:Mn nanoparticles were diluted and placed in cuvette. The absorbance value at 306 and 266 nm corresponding to ZnS:Mn and 5-FU were recorded.

2.6.5. Fluorescence spectroscopy

The fluorescence studies were carried out using Shimadzu Spectrofluorimeter (HORIBA JOBIN YVON Fluoromax-4). The fluorescence emission spectra of 5-FU encapsulated FA–CMC–ZnS:Mn,

FA–CMC–ZnS:Mn and CMC–ZnS:Mn nanoparticles were studied. The nanoparticle sample diluted and placed in cuvette. All measurements were made at the front surfaces of the samples at 45° position with an excitation wavelength of 365 nm and the slit width kept at 5 nm for both excitation and emission. The emission intensities at 598 nm were recorded.

2.6.6. X-ray diffraction

The X-ray diffraction (XRD) experiments were carried out using XRD instrument (X'Pert PRO PANalytical). 5-FU, 5-FU encapsulated FA–CMC–ZnS:Mn and ZnS:Mn nanoparticles were freezed and lyophilized. Five micro-grams of the powder was taken in the sample holder and XRD was recorded.

2.6.7. Fourier transform infrared spectroscopy

Fourier transform infrared (FTIR) spectra of CMC, CMC nanoparticle, 5-FU encapsulated FA–CMC–ZnS:Mn, bare FA and 5-FU were taken. Samples were freezed, lyophilized and their FT-IR spectra were recorded using FTIR spectrophotometer (Perkin Elmer Spectrum RXI). The characteristic peaks were recorded for each sample.

2.7. In vitro drug release

Drug release profile of 5-FU from nanoparticles was carried out in of PBS medium with pH 7.4. Five micro-grams of lyophilized nanoparticles were dispersed in 30 ml of PBS and placed in a water bath shaker set at 37 °C with a shaking speed of 120 rpm. At predetermined time intervals 3 ml of supernatant from the sample was taken for analysis and same amount of fresh PBS was replaced to the sample. Each time the absorbance value at 266 nm was recorded using a UV Spectrophotometer.

$$\text{Drug release } (\%) = \frac{[\text{5-FU}]_{\text{rel}}}{[\text{5-FU}]_{\text{tot}}} \times 100$$

where $[\text{5-FU}]_{\text{rel}}$ is the concentration of released 5-FU collected at time, t and $[\text{5-FU}]_{\text{tot}}$ is the total amount of 5-FU entrapped in the nanoparticles.

2.8. Cell culture

Breast cancer cells line MCF-7 and Mouse fibroblast cells L929 were routinely grown in Minimal essential medium (MEM) with 10% heat-inactivated fetal bovine serum and (100units/ml) penicillin/streptomycin at 37 °C in a humidified 5% CO_2 atmosphere. A stock solution of the nanoparticles sample were prepared and diluted to different concentrations using PBS (pH 7.2) for treatment. Treatments were carried out in 96 well tissue culture plates.

2.8.1. In vitro cytotoxicity studies

MCF-7 cell line was routinely cultured in a humidified temperature with 5% CO_2 in flasks containing medium courtesy. Mouse fibroblast cell line was also maintained in the same way. MTT tests on both these cell lines were done with different concentrations of nanoparticles.

2.8.2. Cell imaging studies

Breast cancer cells MCF-7 grown in a folate free minimal essential medium and MEM supplemented with 10% heat-inactivated fetal bovine serum, 100 units/ml) penicillin/streptomycin at 37 °C under 5% CO_2 were used for the study. The cells were washed with PBS and seeded at two different densities 2×10^4 and 3×10^3 per well onto cover glasses inside a 24-well tissue culture plate. Cells were cultured for 24 h before treating with nanoparticles. The cells were washed again with PBS and media is replaced containing nanoparticles and was incubated for 1 h at 37 °C. Cells were then washed with PBS and fixed with 2% formaldehyde and mounted with mounting medium. Nanoparticles labeled MCF-7 cells were imaged on an Olympus BX-51 fluorescent microscope equipped with a CCD camera and 60×, 100×, 20×, oil immersion objectives. The fluorescence of the nanoparticles was detected using band-pass excitation and emission filters (BP 330–385 nm excitation, 420 nm emission, 400 nm dichromatic mirror).

3. Results and discussion

3.1. Preparation of nanoparticles

The cross-linking of CMC nanoparticles occurs due to the ionic interaction between Ca^{2+} ions and free COO^- groups of the folate conjugated CMC. The cross-linking agent $CaCl_2$ was biocompatible, since calcium is an essential element for our body. Minimum size was obtained with the lowest CMC concentration and the mean size and size distribution increased with increase in concentration of either CMC or $CaCl_2$. For ZnS:Mn preparation 10%, 15% and 20% Mn doping concentrations were done and 15% doping was selected because that gave very good fluorescence. The bright luminescence of the nanoparticles was due to doping of Zn^{2+} with Mn^{2+}. It was found that the microwave irradiation of the sample improved the fluorescence because maximum doping was achieved by the microwave irradiation. The FA–CMC and ZnS:Mn interaction was due to the coordinate bond formed between COO^- groups of FA–CMC to Zn^{2+} with Mn^{2+}. The FA conjugation to CMC was achieved by the formation of –CO–NH– bond formed by the reaction between –COOH and $–NH_2$ groups. EDC and NHS catalyzed the bond formation. The 5-FU encapsulated FA–CMC–ZnS:Mn nanoparticle suspension was kept at room temperature for one month and there was no significant change in particle size or settling down of particles throughout the period. The high stability observed may be due to the electrostatic repulsion between the positively charged nanoparticles.

3.2. Characterization of the prepared nanoparticles

3.2.1. Surface morphology

The surface morphology of nanoparticles was studied using SEM and AFM. Fig. 1 shows the SEM images of FA–CMC–ZnS:Mn nanoparticles and the nanoparticles were found to be spherical in shape. The SEM pictures showed that the 5-FU encapsulated FA–CMC–ZnS:Mn nanoparticles were found to be in the size range of 130–150 nm. The nanoparticles posses average size in the range

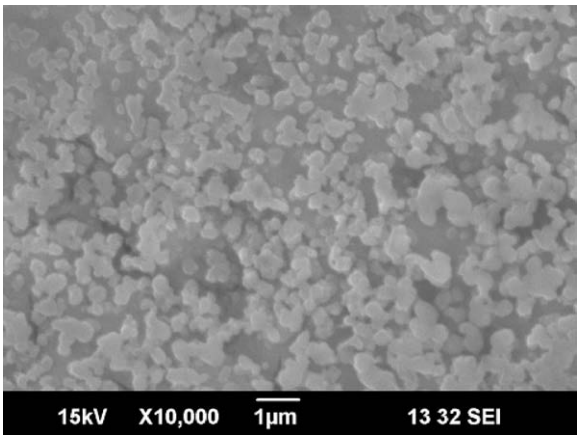

Fig. 1. SEM image of 5-FU encapsulated FA–CMC–ZnS:Mn nanoparticles.

of 60–120 nm. The surface morphology of 5-FU encapsulated FA–CMC–ZnS:Mn nanoparticles were characterized using AFM. The particle size obtained from AFM was 50 nm. Both SEM and AFM images showed that the 5-FU encapsulated FA–CMC–ZnS:Mn nanoparticles were spherical in shape.

3.2.2. Particle size and surface charge analysis

The DLS experiments were carried out at 22 °C. The mean diameter obtained for FA–CMC, 5-FU encapsulated FA–CMC and 5-FU encapsulated FA–CMC–ZnS:Mn nanoparticles were 44, 50 and 79 nm respectively. The encapsulation of the 5-FU slightly increased the size of nanoparticles. The coordination of ZnS:Mn to 5-FU encapsulated FA–CMC again increased the size of the nanoparticles.

The zeta potential is an important index for the stability of nanoparticle suspension. The zeta potential was found to be +36.78 mV for 5-FU encapsulated FA–CMC–ZnS:Mn, indicated good stability. It has been reported that the value of zeta potential less than −30 mV or higher than +30 mV can be used to assure the stability of nanoparticle suspensions. The values obtained for the prepared nanoparticles were above +30, so it was stable. The positive values obtained for zeta potential indicated that the nanoparticle surface was positively charged. This may be due to the availability of free NH_3^+ groups on the polymer. In aqueous solution the carboxyl groups of CMC existed as $-COO^-$ and $-NH_2$ group as $-NH_3^+$. The $-COO^-$ groups get electrostatically bonded to Ca^{2+} ions and the NH_3^+ groups were freely available. It was found that the surface charge increased with increase in concentration of CMC.

3.2.3. Absorbance spectrum

The absorbance spectra of 5-FU encapsulated FA–CMC–ZnS:Mn nanoparticles showed two absorbance peaks with absorbance maxima at 266 and 318 nm, characteristic of 5-FU and ZnS:Mn. The UV absorbance of folic acid was found to be at 280 nm. The absorbance spectrum with peak maximum at 266 nm was a broadened one, which covers the UV absorbance of 5-FU and folic acid. The absorbance spectrum confirmed the encapsulation of the 5-FU, conjugation of FA and coordination of ZnS:Mn because the spectrum contained the characteristic UV absorbance peaks of encapsulated 5-FU, folic acid and ZnS:Mn.

3.2.4. Photoluminescence spectra

Fig. 2A shows the photoluminescence spectra of CMC–ZnS:Mn, FA–CMC–ZnS:Mn and 5-FU encapsulated FA–CMC–ZnS:Mn nanoparticles. The photoluminescence spectra showed that there was a quenching of fluorescence on conjugation with FA. There was again a further reduction of luminescence after the encapsulation of 5-FU to the nanoparticles. The photoluminescence spectrum was taken to study the effect fluorescence of CMC–ZnS:Mn due to conjugation of FA to CMC–ZnS:Mn and encapsulation of 5-FU to FA–CMC–ZnS:Mn. These studies (Fig. 2B) showed that there was a slight intensity reduction for the emission peak obtained for FA–CMC–ZnS:Mn nanoparticles than the CMC–ZnS:Mn. The electronic transitions inside the d levels of the Mn^{2+} metal ion were responsible for the bright luminescence. This may be due to the coordinate bond formed between the –COOH groups of FA–CMC to the metal ions Zn^{2+} and Mn^{2+}. With increase in coordination to Mn^{2+} and Zn^{2+} metal ions of the QD there may be reduction in fluorescence intensity. The encapsulation of 5-FU resulted in further reduction of luminescence intensity. The emission maximum was found to be at 598 nm for CMC–ZnS:Mn, FA–CMC–ZnS:Mn and 5-FU encapsulated FA–CMC–ZnS:Mn. The emission at 598 nm was due to the $^4T_1 \geqslant {}^6A_1$ transition in Mn^{2+}.

Fig. 2B shows the optical photograph of 5-FU encapsulated FA–CMC–ZnS:Mn nanoparticles. It can be seen that the nanoparticles were luminescent even after folate conjugation and 5-Fu encapsulation.

3.2.5. FTIR studies

Fig. 3 shows the FTIR spectra of 5-FU encapsulated FA–CMC–ZnS:Mn nanoparticles, CMC nanoparticle, CMC, bare FA and 5-FU. The FTIR spectra were used to confirm the encapsulation of 5-FU in the nanocarrier. The interaction between 5-FU and FA–CMC was due to the formation of inter molecular hydrogen bond between the –CO group of 5-FU and free –OH group of CMC. Since there is a strong interaction the peak at 1723 cm^{-1} for –CO group disappears in spectra for FA–CMC–ZnS:Mn nanoparticles. Since there is no interaction between the –NH group of 5-FU and CMC the –NH bending peak at 1398 cm^{-1} appears as such in spectra for FA–CMC–ZnS:Mn nanoparticles. These results confirmed the encapsulation of 5-FU in CMC. The $-NH_2$ group in FA shows the –NH stretching vibrations at 1605 cm^{-1}. Since the $-NH_2$ group in FA has no interaction with 5-FU or CMC, the peak appears as such. This can be taken as an indication of FA conjugation to CMC.

3.3. In vitro drug release studies

The drug encapsulation efficiency of FA–CMC–ZnS:Mn nanoparticles were found to be 92.08%. The *in vitro* drug release was studied with PBS at pH 7.4. The percentage of drug released from FA–CMC–ZnS:Mn nanoparticles at predetermined time intervals were calculated using the standard curve prepared for 5-FU. Fig. 4 shows the *in vitro* drug release profile of FA–CMC–ZnS:Mn nanoparticles. The *in vitro* dug release profile (Fig. 4) showed that

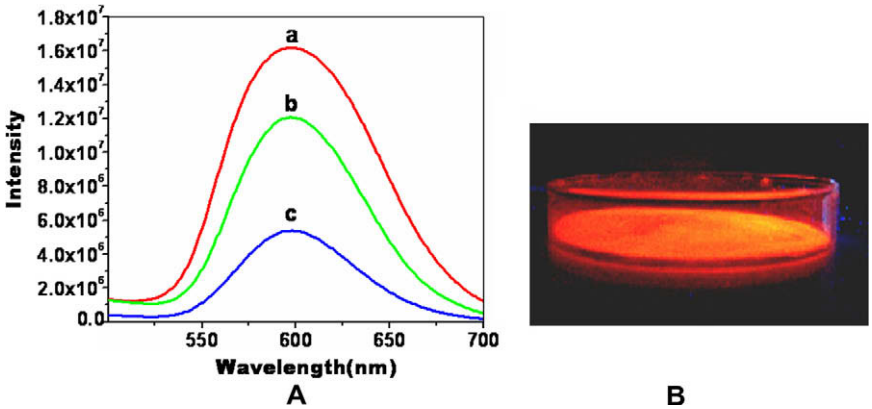

Fig. 2. (A) Photoluminescence spectra of (a) CMC–ZnS:Mn, (b) FA–CMC–ZnS:Mn and (c) 5-FU encapsulated FA–CMC–ZnS:Mn nanoparticles and (B) Optical photograph of 5-FU encapsulated FA–CMC–ZnS:Mn nanoparticles.

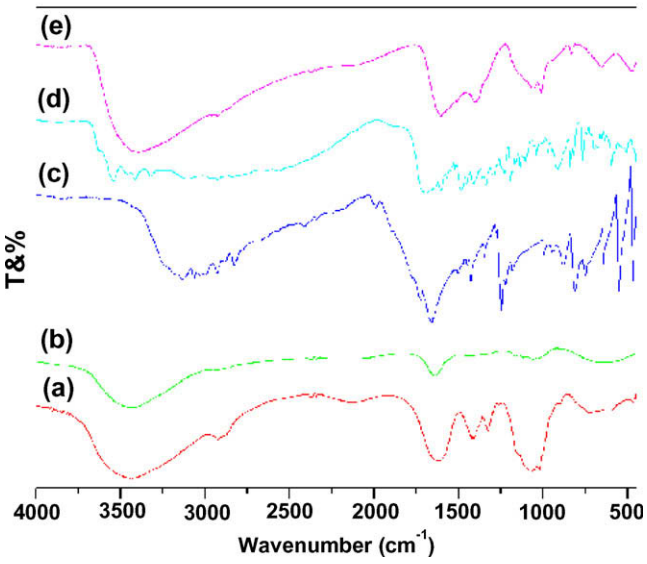

Fig. 3. FTIR spectra of (a) bare CMC, (b) CMC nanoparticles, (c) 5-FU, (d) bare FA and (e) 5-FU encapsulated FA–CMC–ZnS:Mn nanoparticles.

18% of drug was released after 24 h. After the initial burst, a slow release was observed. Very controlled release was observed for a period of twelve days. Eighty-six percent of the encapsulated drug released during this period. A plateau was obtained after six days. FA–CMC–ZnS:Mn nanoparticle was a complex system, so that CMC degraded very slowly and released the drug in a sustained manner. The observed very slow release was significant because controlled release is required in the field of cancer therapy. These results indicated that the FA–CMC–ZnS:Mn nanoparticles are useful controlled delivery system for cancer treatment.

3.4. In vitro cytotoxicity studies

Two sets of MTT were performed to study the cytotoxicity of the nanoparticles. The first one to identify whether the FA–CMC–ZnS:Mn nanoparticles had any toxicity on L929 mouse fibroblast cell lines. The MTT assay of FA–CMC–ZnS:Mn nanoparticles with L929 cells (Fig. 5), was studied using normal tissue cultured wells with out any nanoparticles as negative control and Triton × 100 as positive control. A decrease in OD value means decrease in number

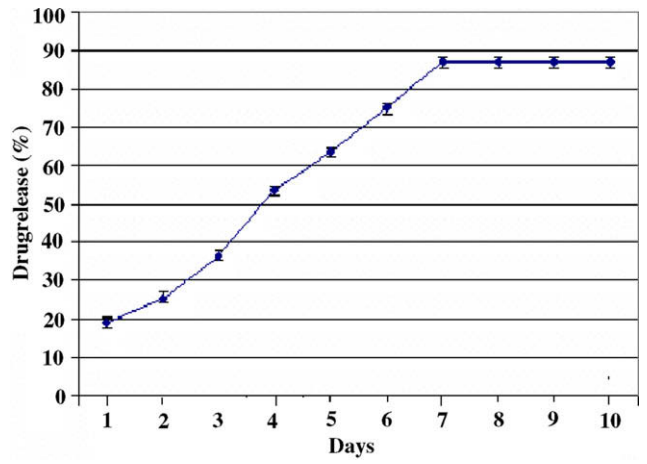

Fig. 4. The *in vitro* release behavior of 5-FU from FA–CMC–ZnS:Mn nanoparticles in PBS (pH 7.4).

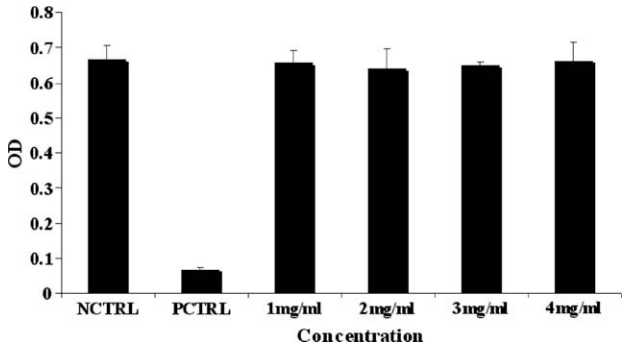

Fig. 5. The MTT cell viability assay of FA–CMC–ZnS:Mn nanoparticles on mouse fibroblast L929 cells.

of viable cells. The results showed that there was no reduction of OD value up to increase of concentration of nanoparticle from 1 mg/ml to 4 mg/ml. Since there was no reduction of live cells on treatment with nanoparticles, it was clear that the FA–CMC–ZnS:Mn nanoparticles were nontoxic to L929 cells.

The second one performed on MCF-7 breast cancer cells line with 5-FU encapsulated FA–CMC–ZnS:Mn nanoparticles. Fig. 6 shows MTT cell viability assay of 5-FU encapsulated FA–CMC–ZnS:Mn nanoparticles treated with MCF-7 cell line. There was reduction in cell viability as the nanoparticle concentration increased from 25% to 100%. There was significant reduction of live cells as the concentration increased to 100%. In the MTT assay of 5-FU encapsulated FA–CMC–ZnS:Mn nanoparticles with MCF-7 cell lines it can be seen that as the concentration of 5-FU encapsulated nanoparticles increased, there was reduction in OD value corresponding to the reduction in number of live cells (Fig. 6). These results clearly indicated that 5-FU encapsulated FA–CMC–ZnS:Mn nanoparticles were able to induce cytotoxic response to MCF-7 cell lines. As the concentration of nanoparticles increased, the concentration of delivered 5-FU also increased which was responsible for more cell death. From the results it was clear that 5-FU encapsulated FA–CMC–ZnS:Mn nanoparticles were causing cytotoxicity and the FA–CMC–ZnS:Mn nanoparticles were cytocompatible.

3.5. In vitro imaging studies

The *in vitro* imaging studies were done on breast cancer cell line MCF-7 that express folate receptors on their surface. The imaging studies (Fig. 7) showed that 5-FU encapsulated FA–CMC–ZnS:Mn nanoparticles showed specific attachment to MCF-7 cells expressing folate receptors at their surface. The control experiments were

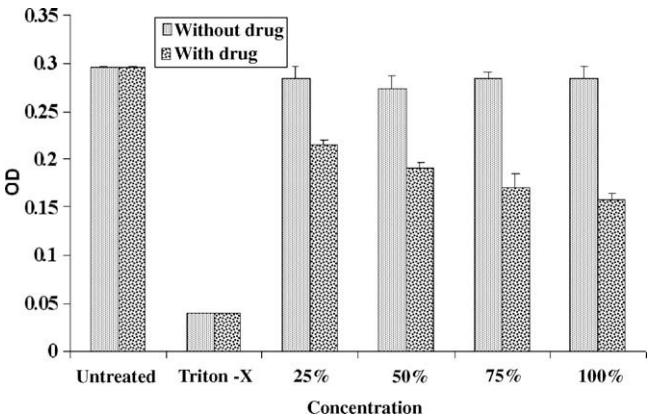

Fig. 6. MTT Cell viability assay of 5-FU encapsulated FA–CMC–ZnS:Mn nanoparticles on MCF-7 cells.

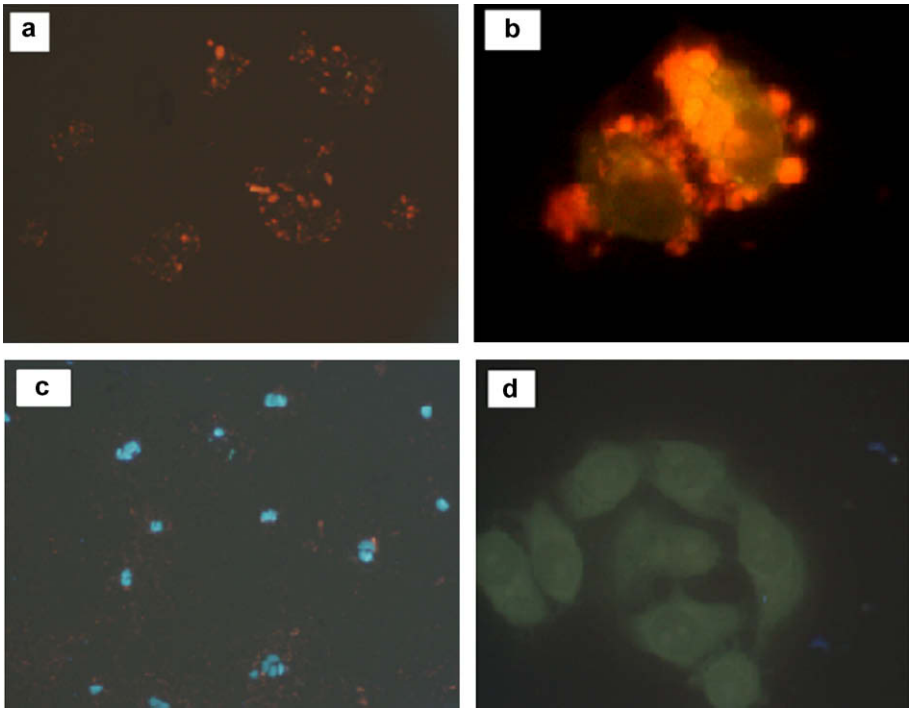

Fig. 7. Images showing interaction of 5-FU encapsulated FA–CMC–ZnS:Mn nanoparticles with (a) MCF-7 cell line (bright field microscopic image), (b) MCF-7 cell line (100× magnification, fluorescent microscopic image), (c) nontargeted 5-FU encapsulated CMC–ZnS:Mn nanoparticles with MCF-7 cell line (10× magnification, fluorescent microscopic image) and (d) MCF-7 cell line alone without nanoparticles (100× magnification, fluorescent microscopic image).

done without folate conjugation showed no specific cell attachment. There was no observed change in cell morphology due to the nanoparticle uptake. From these results the fluorescence from ZnS:Mn can be used for tracking the path of 5-FU encapsulated FA–CMC–ZnS:Mn nanoparticles and FA–CMC–ZnS:Mn nanoparticles alone can be used for targeted imaging of cancer cells.

4. Conclusions

Novel multi-functional FA–CMC–ZnS:Mn nanoparticles were developed by a simple aqueous route. These multi-functional nanoparticles can effectively be used for targeted drug delivery and imaging the path of drug carrier by the fluorescence of ZnS:Mn attached to the system. The prepared nanoparticles were characterized using SEM, AFM, FTIR, UV spectroscopy and Spectroflourimetry. The drug encapsulation efficiency obtained was 92.08% with CMC to 5-FU ratio 2:1. The *in vitro* drug release studies showed controlled release of 5-FU from FA–CMC–ZnS:Mn nanoparticles. The specific targeting and fluorescent imaging with the nanoparticles were studied using breast cancer cell line MCF-7. The FA–CMC–ZnS:Mn nanoparticles were found to be nontoxic to mouse fibroblast L929 cells. But 5-FU encapsulated nanoparticles were found to be toxic to MCF-7 cell line. The nanoparticles without drug encapsulation can be used as a potential bioprobe. This system can also be used for the delivery of genes and proteins with simultaneous imaging.

Acknowledgements

The Department of Science and Technology, Government of India supported this work, under a centre grant of the Nanoscience and Nanotechnology initiative program monitored by Dr. C.N.R. Rao. The author's R. Jayakumar also grateful to Department of Biotechnology (DBT), Govt. of India for providing research support. The authors are also thankful to Mr. Sajin. P. Ravi, Anju R. Babu and Anitha V.C. for their help in SEM and AFM studies.

References

Bhargava, R. N., Gallagher, D., & Welker, T. (1994). Doped nanocrystals of semiconductors – A new class of luminescent materials. *Journal of Luminescence, 60*, 275–280.

Fernando, R. D. A., & Sérgio, P. C. (2004). Characteristics and properties of carboxymethyl chitosan related to the preparation conditions. *Carbohydrate Polymers, 75*, 214–221.

Jabr-Milane, L., Vlerken, L., Devalapally, H., Shenoy, D., Komareddy, S., Bhavsar, M., et al. (2008). Multi-functional nanocarriers for targeted delivery of drugs and genes. *Journal of Controlled Release, 130*, 121–128.

Jayakumar, R., Nme, N., Tokura, S., & Tamura, H. (2007). Sulfated chitin and chitosan as novel biomaterials. *International Journal of Biological Macromolecules, 40*, 175–181.

Jayakumar, R., Prabaharan, M., Reis, R. L., & Mano, J. F. (2005). Graft-copolymerized chitosan – Present status and applications. *Carbohydrate Polymers, 62*, 142–158.

Ke, C., Mathias, C. J., & Green, M. A. (2003). The folate receptor as a molecular target for tumor-selective radionuclide delivery. *Nuclear Medicinal Biology, 30*, 811–817.

Lu, Y., & Low, P. S. (2002). Folate-mediated delivery of macromolecular anticancer therapeutic agents. *Advanced Drug Delivery Reviews, 54*, 675–693.

Manzoor, K., Johny, S., Menon, D., & Nair, S. V. (2009). Bioconjugated luminescent quantum dots of doped ZnS:Mn a cytofriendly system for targeted cancer imaging. *Nanotechnology, 20*, 065102.

Michael, J. M., David, L. S., Eric, C. L., & Christof, A. N. (2008). Fluorescence correlation spectroscopy of CdSe/ZnS quantum dot optical bioimaging probes with ultra thin biocompatible coatings. *Optics Communications, 281*, 1771–1780.

Pan, J., & Feng, S. S. (2009). Targeting and imaging cancer cells by folate decorated quantum dots loaded nanoparticle of biodegradable polymers. *Biomaterials, 30*, 1176–1183.

Prabaharan, M., & Mano, J. F. (2005). Chitosan-based particles for controlled drug delivery systems. *Drug Delivery, 12*, 41–57.

Prabaharan, M. (2008). Chitosan derivatives as promising materials for controlled drug delivery. *Journal of Biomaterials Applications, 23*, 5–36.

Prabaharan, M., Grailer, J. J., Pilla, S., Steeber, D. A., & Gong, S. (2009a). Amphiphilic multi-arm-block copolymer conjugated with doxorubicin via pH-sensitive hydrazone bond for tumor-targeted drug delivery. *Biomaterials, 30*, 5757–5766.

Prabaharan, M., Grailer, J. J., Pilla, S., Steeber, D. A., & Gong, S. (2009b). Gold nanoparticles with a monolayer of doxorubicin-conjugated amphiphilic block copolymer for tumor-targeted intracellular drug delivery. *Biomaterials, 30*, 6065–6075.

Prabaharan, M., Grailer, J. J., Pilla, S., Steeber, D. A., & Gong, S. (2009c). Folate-conjugated amphiphilic hyperbranched block copolymers based on boltorn® H40, poly(L-lactide) and poly(ethylene glycol) for tumor-targeted drug delivery. *Biomaterials, 30*, 3009–3019.

Prabaharan, M., Grailer, J. J., Steeber, D. A., & Gong, S. (2009d). Thermo-sensitive micelles based on folate-conjugated poly(*N*-vinylcaprolactam)-block-

poly(ethylene glycol) copolymers for tumor-targeted drug delivery. *Macromolecular Bioscience, 9*, 744–753.

Saad, M., Garbuzenko, O. B., Ber, E., Chandna, P., Khandare, J. J., Pozharov, V. P., et al. (2008). Receptor targeted polymers, dendrimers, liposomes: Which nanocarrier is the most efficient for tumor-specific treatment and imaging? *Journal of Controlled Release, 130*, 107–114.

Sanvicens, N., & Marco, M. P. (2008). Multifunctional nanoparticles – Properties and prospects for their use in human medicine. *Trends in Biotechnology, 26*, 425–433.

Shi, X., Du, Y., Yang, J., Zhong, B., & Sun, L. (2006). Effect of degree of substitution and molecular weight of carboxymethyl chitosan nanoparticles on doxorubicin delivery. *Journal of Applied Polymer Science, 100*, 4689–4696.

Shen, Y., Zhan, Y., Tang, J., Xu, P., Johnson, P. A., Radosz, M., et al. (2008). Multifunctioning pH-rResponsive nanoparticle from hierarchical self-assembly of polymer brush for cancer drug delivery. *AIChE Journal, 54*, 2979–2989.

Soppimath, K. S., Aminabhavi, T. M., Kulkarni, A. R., & Rudzinski, W. E. (2000). Biodegradable polymeric nanoparticles as drug delivery devices. *Journal of Controlled Release, 70*, 1–20.

Steitz, B., Hofmann, H., Axmann, Y., & Petri-Fink, A. (2008). Optical properties of annealed Mn^{2+} doped ZnS nanoparticles. *Journal of Luminescence, 128*, 92–98.

Vlerken, L., & Amiji, M. (2006). Multi-functional polymeric nanoparticles for tumour-targeted drug delivery. *Expert Opinion in Drug Delivery, 3*, 205–216.

Wu, J., Liu, Q., & Lee, R. J. (2006). A folate receptor-targeted liposomal formulation for paclitaxel. *International Journal of Pharmaceutics, 316*, 148–153.

Xie, M., Liu, H., & Zhan, Z. (2005). CdSe/ZnS-labeled carboxymethyl chitosan as a bioprobe for live cell imaging. *Chemical Communications, 5*, 5518–5520.

Zhu, A., Jin, W., Yuan, L., Yang, G., Yu, H., & Hao, H. (2007). O-carboxymethyl chitosan-based novel gatixoxacin delivery system. *Carbohydrate Polymers, 68*, 693–700.